

THE DISCOVERY OF THE OPTICAL AND NEAR-IR AFTERGLOWS OF THE FIRST *Swift* GAMMA-RAY BURSTS

E. BERGER^{1,2,3}, D. B. FOX⁴, S. R. KULKARNI⁴, W. KRZEMINSKI⁵, A. M. SODERBERG⁴, D. A. FRAIL⁶,
 D. N. BURROWS⁷, S. B. CENKO⁴, E. J. MURPHY⁸, P. A. PRICE⁹, A. GAL-YAM^{4,3}, D.-S. MOON⁴,
 N. GEHRELS¹⁰, W. L. FREEDMAN¹, S. E. PERSSON¹, S. BARTHELMEY¹⁰, J. E. HILL⁷, J. A. NOUSEK⁷,
 A. MORETTI¹¹

Draft version August 27, 2018

ABSTRACT

We present optical and near-infrared searches for afterglow emission from the first four *Swift* bursts with accurate positions from the X-ray Telescope (XRT). Using telescopes at Las Campanas, Keck, and Palomar observatories we rapidly identified and followed up afterglows for three of the four bursts. The burst positions were also observed with the Very Large Array, but no radio afterglow emission was detected. The optical/NIR afterglows are fainter than about 75% of all afterglows detected to date, with GRB 050126 being the faintest, and were identified thanks to accurate and rapid positions from the XRT and rapid response with $\gtrsim 1$ -m telescopes. This suggests that the fraction of dust-obscured bursts is small, $\lesssim 10\%$ when combined with afterglows localized by the HETE-2 Soft X-ray Camera. The X-ray fluxes are typical of the known population, with the exception of GRB 050126 which has the faintest X-ray afterglow to date (normalized to $\Delta t = 10$ hr), and was detected thanks to a response time of only 130 s after the burst. Finally, we find that all three optical/NIR afterglows are located $\lesssim 2$ arcsec away from the nominal XRT positions, suggesting that the XRT is capable of delivering highly accurate positions, which will revolutionize afterglow studies.

Subject headings: gamma-rays:bursts

1. INTRODUCTION

The *Swift* γ -ray satellite (Gehrels *et al.* 2004), launched on 2004, November 20, holds great promise for our understanding of γ -ray bursts (GRBs), as well as their use for cosmological applications. This is primarily because of the positional accuracy and great sensitivity of the Burst Alert Telescope (BAT), and the on-board X-ray telescope (XRT) and UV/optical telescope (UVOT), which are capable of providing ~ 0.3 – 5 arcsec positions and detailed light curves within a few minutes after the burst. Starting in mid-December 2004 *Swift* has localized several bursts of which a few have been followed up with the XRT providing ~ 8 – 30 arcsec error circles on a timescale of several hours. The rapidity and accuracy of these localizations have enabled deep ground-based optical and near-infrared (NIR) searches.

Here we present a comprehensive investigation (optical, near-IR, radio) of the first four *Swift* bursts with XRT detections: GRBs 041223, 050117a, 050124 and 050126. The observations were conducted at Las Campanas Observatory (LCO), Palomar Observatory, Keck Observatory and the Very Large Array (VLA). Even at this early stage, with the localization timescale and accuracy still an order of magnitude below the eventual capability of *Swift*, the combination of *Swift* and $\gtrsim 1$ -

m class ground-based telescopes suggests that the fraction of dust-obscured GRBs is likely low, and the afterglow recovery rate for *Swift* bursts may approach unity.

2. AFTERGLOW IDENTIFICATION AND FOLLOW-UP OF *Swift* GAMMA-RAY BURSTS

2.1. GRB 041223

The *Swift* Burst Alert Telescope (BAT) localized this burst on 2004, December 23.5877 UT to a $7'$ radius error circle (Tueller *et al.* 2004; Markwardt *et al.* 2004). A series of XRT observations was initiated on December 23.780 UT, and a fading source was detected at $\alpha=06^{\text{h}}40^{\text{m}}49.2^{\text{s}}$, $\delta=-37^{\circ}04'21.5''$ (J2000) with an uncertainty of about $15''$ radius (Burrows *et al.* 2004). The spectral energy index was $\beta_x = -1.02 \pm 0.13$ and the temporal decay rate was about $\alpha_x = -1.7 \pm 0.2$ ($F_\nu \propto t^{\alpha_x} \nu^{\beta}$) with a flux of 6.5×10^{-12} erg cm⁻² s⁻¹ (0.5 – 10 keV) about 6.2 hr after the burst (Table 1; Burrows *et al.* 2005a). Following our discovery of the optical transient, the XRT position was revised to (Tagliaferri *et al.* 2004) $\alpha=06^{\text{h}}40^{\text{m}}47.4^{\text{s}}$, $\delta=-37^{\circ}04'22.3''$ (J2000), within about $1''$ of the optical afterglow position.

Ground-based observations commenced on December 24.185 UT (14.4 hours after the burst) using the Swope 40-in telescope at LCO (Berger, Krzeminski & Hamuy 2004). We

¹Observatories of the Carnegie Institution of Washington, 813 Santa Barbara Street, Pasadena, CA 91101

²Princeton University Observatory, Peyton Hall, Ivy Lane, Princeton, NJ 08544

³Hubble Fellow

⁴Division of Physics, Mathematics and Astronomy, 105-24, California Institute of Technology, Pasadena, CA 91125

⁵Las Campanas Observatory, Carnegie Observatories, Casilla 601, La Serena, Chile

⁶National Radio Astronomy Observatory, Socorro, NM 87801

⁷Department of Astronomy and Astrophysics, Pennsylvania State University, 525 Davey Laboratory, University Park, PA 16802

⁸Department of Astronomy, Yale University, P.O. Box 208101, New Haven, CT 06520-8101

⁹Institute for Astronomy, University of Hawaii, 2680 Woodlawn Drive, Honolulu, HI 96822

¹⁰NASA Goddard Space Flight Center, Greenbelt, MD 20771

¹¹INAF – Osservatorio Astronomico di Brera, Via Bianchi 46, 23807 Merate, Italy

imaged the entire $7'$ radius BAT error circle in the r -band for a total of 20 min. The data were bias-subtracted, flat-fielded, and combined using standard IRAF routines. Astrometry was performed relative to the USNO-B catalog using 200 stars in common to the two frames. The resulting rms positional uncertainty was $0.15''$. A stationary source not present in the Digital Sky Survey (DSS) was detected at $\alpha=06^{\text{h}}40^{\text{m}}47.323^{\text{s}}$, $\delta=-37^{\circ}04'22.77''$ (J2000) with a magnitude of $r \approx 21 \pm 0.15$. This position was $7.5''$ outside of the initial XRT error circle, but only $1''$ from the revised nominal XRT position. A field centered on the position of the afterglow of GRB 041223 is shown in Figure 1, and the observations are summarized in Table 2.

Additional observations with the Swope 40-in telescope were obtained starting on December 25.15 UT in the r and i bands. A total of 1 hr was obtained in each filter. A comparison of the first and second epoch indicated that the afterglow had faded by 1.2 mag, corresponding to a decay rate of $\alpha \approx -1.1$.

We subsequently observed the position of the afterglow with the Low-Resolution Imager and Spectrograph (LRIS; Oke *et al.* 1995) mounted on the Keck-I 10-m telescope on 2005, January 8.34 UT. We obtained R -band observations for a total of 70 min. The data were reduced and analyzed in the manner described above. These observations reveal a faint source at the position of the afterglow with $R \approx 24.5 \pm 0.3$ mag. An extrapolation of the afterglow flux at $t = 1.56$ d to the epoch of the LRIS observation suggests that this object is most likely the afterglow, although any steepening in the afterglow evolution (e.g., jet break) would mean that the emission is dominated by the host galaxy.

Late-time observations were obtained with the Near Infra-Red Camera (NIRC; Matthews & Soifer 1994) mounted on the Keck-I telescope in the K_s -band on 2005, January 25.33 UT. A total of sixty-two 50-s images were collected. The individual images were dark-subtracted, flat-fielded, and corrected for bad pixels and cosmic rays. We then created object masks, which were used to construct improved flat fields for a second round of reduction. The data were finally registered, shifted, and co-added. Photometry was performed relative to three 2MASS sources in the field, and no object was detected at the position of the afterglow to a 3σ limit of $K_s = 22.0$ mag.

Finally, we obtained spectroscopic observations using LRIS with a 400-line grating on the red side (dispersion of 1.86 \AA/pix) and a 600-line grism on the blue side (dispersion of 0.63 \AA/pix). Two 2400 s exposures were obtained with a $1.5''$ slit. The data were bias-subtracted and flat-fielded using IRAF. Rectification and sky subtraction were performed using the method and software described in Kelson (2003). We detect weak continuum emission, but no obvious emission lines in the range $\approx 3500 - 9500 \text{ \AA}$.

2.2. GRB 050117a

This burst was localized by the BAT on 2005, January 17.5365 UT to a $4'$ radius error circle (Sakamoto *et al.* 2005; Barthelmy *et al.* 2005). XRT observations revealed a fading source at $\alpha=23^{\text{h}}53^{\text{m}}53.0^{\text{s}}$, $\delta=+65^{\circ}56'20''$ (J2000) with an uncertainty of $15''$ radius (Hill *et al.* 2005b). We note that the location of GRB 050117a less than 4° away from the Galactic plane results in large extinction, $E(B-V) = 1.75$ mag (Schlegel, Finkbeiner & Davis 1998), which severely hampered optical searches.

We observed the XRT position of GRB 050117a with the Wide Field Infra-red Camera (WIRC) mounted on the Palomar Hale 200-in telescope on January 18.146 UT (14.6 hrs after the burst; Fox, Cenko & Murphy 2005). A total of 32 min were obtained in the K_s band. Several 2MASS and DSS sources were detected within and near the XRT position. A field centered on the XRT error circle of GRB 050117a is shown in Figure 2. At the present no afterglow candidate is identified.

We observed the field with the VLA¹² on 2005, January 19.08 and 24.14 UT (1.54 and 6.60 days after the burst, respectively) at a frequency of 8.46 GHz (Frail 2005; Soderberg & Frail 2005b). No source was detected within the error circle to a 3σ limit of 98 (Jan. 19.08) and 84 (Jan. 24.14) μJy .

2.3. GRB 050124

This burst was localized by the BAT on 2005, January 24.4792 UT to a $6'$ radius error circle (Markwardt *et al.* 2005; Cummings *et al.* 2005). An XRT observation was initiated on January 24.607 UT (3.1 hr after the burst), and ground analysis revealed a source at $\alpha=12^{\text{h}}51^{\text{m}}30.4^{\text{s}}$, $\delta=+13^{\circ}02'39.0''$ (J2000), with an uncertainty of $8''$ (Pagani *et al.* 2005). The flux of the source was $2 \times 10^{-12} \text{ erg cm}^{-2} \text{ s}^{-1}$ (2–10 keV).

We observed the XRT $8''$ error circle with NIRC in the J and K_s bands starting on January 25.501 (24.5 hrs after the burst; Berger & Kulkarni 2005a). A total of 15 min were obtained in each band. Within the XRT error circle we detected a single point source, located at $\alpha=12^{\text{h}}51^{\text{m}}30.35^{\text{s}}$, $\delta=+13^{\circ}02'41.3''$ (J2000). The astrometry was performed relative to an image of the field from the Palomar 60-in telescope with an rms positional uncertainty of $0.2''$. The NIR afterglow position is only $2.4''$ away from the nominal XRT position. Follow-up observations with NIRC on January 26.471 (47.8 hours after the burst) in the J (13.3 min) and K_s (14.2 min) bands revealed a clear fading of the point source confirming its identification as the afterglow of GRB 050124 (Berger & Kulkarni 2005b). The brightness of the source was $K_s = 19.66 \pm 0.06$ mag in the first observation. The observations are summarized in Table 2 and the first epoch NIRC image is shown in Figure 3.

Observations were conducted with the VLA at 4.86 and 8.46 GHz on 2005, January 29.41 UT (4.93 days after the burst; Soderberg & Frail 2005a). No source was detected at the position of the NIR afterglow, or within the XRT position, to a 3σ limit of 130 (4.86 GHz) and 100 (8.46 GHz) μJy .

2.4. GRB 050126

This burst was localized with the BAT on 2005, January 26.5001 UT to a $4'$ radius error circle (Sato *et al.* 2005). The XRT observation started 129 s after the burst and revealed a source which was localized to a $30''$ error circle. Ground analysis based on data from four orbits resulted in a refined position of $8''$ accuracy (Campana *et al.* 2005) centered on $\alpha=18^{\text{h}}32^{\text{m}}27.0^{\text{s}}$, $\delta=+42^{\circ}22'13.5''$ (J2000).

We observed the XRT $30''$ error circle with NIRC in the K_s band starting on 2005, January 26.682 UT (4.4 hours after the burst; Berger & Kulkarni 2005c,d) for a total of 8.3 min. The data were reduced in the manner outlined above, and astrometry was performed relative to the DSS using six stars in common between the two images. The resulting rms positional uncertainty was $0.12''$. Within the revised XRT error circle we detect one object not visible in the DSS at $\alpha=18^{\text{h}}32^{\text{m}}27.18^{\text{s}}$,

¹²The VLA is operated by the National Radio Astronomy Observatory, a facility of the National Science Foundation operated under cooperative agreement by Associated Universities, Inc.

$\delta = +42^\circ 22' 13.6''$ (J2000). This position is only $2.0''$ away from the nominal XRT position. The source has $K_s = 19.45 \pm 0.17$ mag. The NIRC image is shown in Figure 4. We note that while this is the only candidate in the XRT error circle, we have been unable to confirm that the object has actually faded. If this is in fact not the NIR afterglow, then this is by far the faintest limit for any afterglow observed to date (see Figure 5 and Klose *et al.* 2003).

We observed the position of GRB 050126 with the VLA at 8.46 GHz on 2005, January 26.67 and 28.59 UT (4.1 hr and 2.09 d after the burst, respectively). No object was detected at the position of the NIR candidate or within the revised XRT error circle to a limit of about $100 \mu\text{Jy}$ (Frail & Soderberg 2005).

3. AFTERGLOW PROPERTIES

We now provide a simple analysis of the afterglow emission from the individual bursts. For GRB 041223 we combine the data presented in this paper with measurements in the J - and K -band from Burrows *et al.* (2005a). Correcting for Galactic extinction ($A_R = 0.32$, $A_I = 0.23$, $A_J = 0.11$, and $A_K = 0.04$ mag; Schlegel, Finkbeiner & Davis 1998) we find that the best-fit spectral index using all the available observations is $\beta = -0.6 \pm 0.1$, while the best-fit temporal decay rate is $\alpha = -1.1 \pm 0.1$. In the absence of significant extinction within the host galaxy, we can use these values, along with the synchrotron closure relations (e.g. Berger *et al.* 2002), to determine the value of the electron distribution power law index, p ($N(\gamma) \propto \gamma^{-p}$), the geometry of the circumburst environment (ISM or Wind), and the location of the synchrotron cooling frequency relative to the optical/NIR band. Three possibilities exist, namely $\alpha - 3\beta/2 = 0$ (ISM_b), $\alpha - 3\beta/2 - 1/2 = 0$ (ISM_r and Wind_r), and $\alpha - 3\beta/2 + 1/2 = 0$ (Wind_b); the subscript designates whether the cooling frequency is blueward (b) or redward (r) of the optical/NIR band. The ISM_b closure relation provides the best result, -0.2 ± 0.25 , indicating that $p \approx 2.2 \pm 0.2$, and the cooling frequency is located blueward of the optical/NIR band. This conclusion is supported by the X-ray spectral index, $\beta_x \approx -1 \pm 0.1$, which indicates $p \approx 2 \pm 0.2$.

A comparison of the optical/NIR flux and the X-ray flux, extrapolated to a common time of 19.6 hr using $\alpha_x = -1.7$, indicates that $\beta_{ox} \approx -0.65$. Taken in conjunction with the optical and X-ray spectral indices, this indicates that the cooling frequency is $\nu_c \approx 1.1 \times 10^{17}$ Hz or about 0.45 keV. We note, however, that in the context of this model, the X-ray temporal decay is expected to be $\alpha_x \approx -1.1 \pm 0.1$, which is about 2.7σ away from the measured value, $\alpha_x \approx -1.7 \pm 0.2$. The steeper decay may be due to a contribution from inverse Compton emission (Sari & Esin 2001). We note that Burrows *et al.* (2005a) suggest that the optical/NIR and X-ray afterglows are dominated by two different physical components.

We perform a similar analysis for GRB 050124. Based on the pair of J - and K_s -band observations taken on the first and second nights after the burst, we find a spectral index, $\beta \approx 0.4 \pm 0.2$, and a temporal decay index $\alpha \approx 1.45 \pm 0.25$. These values satisfy the closure relation for the Wind_b case, -0.35 ± 0.55 , indicating that $p \approx 2.1 \pm 0.3$ and the cooling frequency is located blueward of the NIR bands. A comparison of the X-ray flux at 7.1 hours after the burst to the NIR flux, extrapolated to the epoch of the X-ray observations using the measured value of α , indicates an optical/X-ray spectral index, $\beta_{ox} \approx -0.5$, in good agreement with the optical/NIR spectral index. This suggests that the cooling break is most likely located near the X-ray band.

Finally, for GRB 050126 we simply note that both the NIR and X-ray afterglows are fainter than any other afterglow detected to date. For the purpose of this comparison we extrapolate the NIR flux to the optical R -band using a typical spectral index of -0.6 , and the X-ray flux from 200 s to 10 hr using $\alpha_x \approx -1.3$, which is typical for X-ray afterglows (Berger, Kulkarni & Frail 2003).

4. DISCUSSION AND CONCLUSIONS

One of the main promises of *Swift* is rapid localization and follow-up with the XRT and UVOT. The X-ray fluxes from XRT (Burrows *et al.* 2005a; Hill *et al.* 2005a; Osborne *et al.* 2005a; Tagliaferri *et al.* 2005) are summarized in §2 and Table 1. In Figure 5 we plot the X-ray fluxes normalized to 10 hours after the burst in comparison to the sample of Berger, Kulkarni & Frail (2003). We find that three of the four XRT afterglows are typical of the general population, but the X-ray afterglow of GRB 050126 is the faintest detected to date (when normalized to 10 hrs), and it was only detected thanks to the rapid response of the XRT. The fluxes were extrapolated to the common epoch using the measured temporal decay index or the typical $F_\nu \propto t^{-1.3}$ (Berger, Kulkarni & Frail 2003). We note that the X-ray flux for GRB 050117a is dominated by the prompt emission and should be considered an upper limit.

Similarly, we plot the R -band magnitudes of the *Swift* afterglows, measured directly or extrapolated from the NIR (using the measured spectral indices or a typical $F_\nu \propto \nu^{-0.6}$), in comparison to a compilation of optical light curves collected in the past seven years. We find that the afterglows are fainter than about 75% of the population on a similar timescale (Figure 5). In particular, the possible afterglow of GRB 050126 is the faintest detected to date. The afterglow detections are due to the accurate positions available from the XRT which allowed us to both identify the afterglows more readily, and to search the error circles in the NIR with a large aperture telescope. We note that the faintness of the optical afterglows may also explain the non-detections in the radio.

Several conclusions can already be drawn from this early work. First, nearly every XRT localization has resulted in the identification of an optical or NIR afterglow; the single exception (GRB 050117a) is likely due to large Galactic extinction. The optical/NIR afterglow recovery rate for XRT (3/4) and the HETE-2 SXC (12/13) is $\gtrsim 90\%$. The brightness of the XRT+SXC sample normalized to $t = 12$ hr compared to all other optical afterglows is shown in Figure 6. The afterglows of the XRT bursts appear to be fainter than about 75% of all afterglows detected prior to *Swift*, suggesting that past non-detections were mainly the result of large error regions and/or shallow searches. This indicates that the fraction of “dark” (dust-obscured) GRBs is low, although we note that two of the XRT bursts were localized in the NIR and may still be dust-obscured. If this trend persists then this bodes well for identification of high redshift afterglows using the Lyman break technique, since the main contaminant is dust-obscured bursts.

Second, in the three cases in which an optical/NIR afterglow was detected, the offset relative to the nominal XRT position has been $\lesssim 2$ arcsec, much less than the size of the error circles. This suggests that in the near future the XRT will be capable of providing ~ 2 arcsec positions. This will significantly reduce the delay from localization to identification of the optical/NIR afterglow in cases when a UVOT sub-arcsecond position is not available.

We end by noting that the faintness of the optical/NIR af-

terglows studied in this paper ($R \approx 18$ mag at $\Delta t = 1$ hr; Figures 5 and 6) may make it difficult for small robotic telescopes to provide long-term follow-up of *Swift* bursts. However, larger telescopes, while somewhat slower to respond, will allow both long-term follow-up and detection of the faintest afterglows, particularly in the NIR.

We thank the staff at the Las Campanas Observatory, the Palomar Observatory, the Keck Observatory, and the Very Large Array. We also thank Mario Hamuy for generous use

of his observing time and Dan Kelson for help with his sky background subtraction software. E.B. is supported by NASA through Hubble Fellowship grant HST-01171.01 awarded by the Space Telescope Science Institute, which is operated by AURA, Inc., for NASA under contract NAS 5-26555. Additional support was provided by NSF and NASA grants. A.G. acknowledges support by NASA through Hubble Fellowship grant HST-HF-01158.01-A awarded by STScI, which is operated by AURA, Inc., for NASA, under contract NAS 5-26555.

References

- Barthelmy, S. *et al.* 2005, GRB Circular Network, 2962, 1.
- Berger, E., Krzeminski, W., and Hamuy, M. 2004, GRB Circular Network, 2902, 1.
- Berger, E. and Kulkarni, S. R. 2005a, GRB Circular Network, 2978, 1.
- Berger, E. and Kulkarni, S. R. 2005b, GRB Circular Network, 2983, 1.
- Berger, E. and Kulkarni, S. R. 2005c, GRB Circular Network, 2985, 1.
- Berger, E. and Kulkarni, S. R. 2005d, GRB Circular Network, 2997, 1.
- Berger, E. *et al.* 2002, ApJ, 581, 981.
- Berger, E., Kulkarni, S. R., and Frail, D. A. 2003, ApJ, 590, 379.
- Burrows, D. N. *et al.* 2005a, ApJ in press.
- Burrows, D. N. *et al.* 2004, GRB Circular Network, 2901, 1.
- Campana, S. *et al.* 2005, GRB Circular Network, 2996, 1.
- Cummings, J. *et al.* 2005, GRB Circular Network, 2973, 1.
- Fox, D. B., Cenko, S. B., and Murphy, E. 2005, GRB Circular Network, 2960, 1.
- Frail, D. A. 2005, GRB Circular Network, 2963, 1.
- Frail, D. A. and Soderberg, A. M. 2005, GRB Circular Network, 2993, 1.
- Gehrels, N. *et al.* 2004, ApJ, 611, 1005.
- Hill, J. E. *et al.* 2005a, in prep.
- Hill, J. E. *et al.* 2005b, GRB Circular Network, 2955, 1.
- Kelson, D. D. 2003, PASP, 115, 688.
- Klose, S. *et al.* 2003, ApJ, 592, 1025.
- Markwardt, C. *et al.* 2004, GRB Circular Network, 2909, 1.
- Markwardt, C. *et al.* 2005, GRB Circular Network, 2972, 1.
- Matthews, K. and Soifer, B. T. 1994, in ASSL Vol. 190: Astronomy with Arrays, The Next Generation, 239.
- Oke, J. B. *et al.* 1995, PASP, 107, 375.
- Osborne, J. P. *et al.* 2005a, in prep.
- Pagani, C. *et al.* 2005, GRB Circular Network, 2974, 1.
- Sakamoto, T. *et al.* 2005, GRB Circular Network, 2952, 1.
- Sari, R. and Esin, A. A. 2001, ApJ, 548, 787.
- Sato, G. *et al.* 2005, GRB Circular Network, 2987, 1.
- Schlegel, D. J., Finkbeiner, D. P., and Davis, M. 1998, ApJ, 500, 525.

- Soderberg, A. M. and Frail, D. A. 2005a, GRB Circular Network, 3000, 1.
- Soderberg, A. M. and Frail, D. A. 2005b, GRB Circular Network, 2980, 1.
- Tagliaferri, G. *et al.* 2005, in prep.
- Tagliaferri, G. *et al.* 2004, GRB Circular Network, 2910, 1.
- Tueller, J. *et al.* 2004, GRB Circular Network, 2898, 1.

TABLE 1
PROMPT EMISSION AND X-RAY AFTERGLOW PROPERTIES

GRB	t_0 (UT)	F (erg cm ⁻²)	t_{90} (s)	α	t_X (s)	F_X (erg cm ⁻² s ⁻¹)	α_X	β_X
041223	23.5877	5×10^{-5}	130	1.1	1.63×10^4	6.5×10^{-12}	-1.72 ± 0.20	-1.02 ± 0.13
050117a	17.5365	1.7×10^{-5}	220	...	193	1.8×10^{-8} ^a
050124	24.4792	2.1×10^{-6}	4.1	1.5	2.54×10^4	2.2×10^{-12}
050126	26.5001	2.0×10^{-6}	26	1.3	200	2.5×10^{-11}

NOTE.—Prompt emission and X-ray afterglow properties of the four bursts discussed in this paper. The columns are (left to right): (i) GRB name, (ii) burst time, (iii) fluence in the 15–350 keV band, (iv) burst duration, (v) spectral index, (vi) time of X-ray observation, (vii) X-ray flux, (viii) X-ray temporal decay index, (ix) X-ray spectral index. ^a The X-ray flux of GRB 050117a is dominated by the prompt emission.

TABLE 2
GROUND-BASED OPTICAL AND NEAR-INFRARED DATA

Date (UT)	Δt (days)	Telescope	Filter	Magnitude
GRB 041223				
2004, Dec. 24.185	0.60	LCO40	<i>r</i>	20.99 ± 0.15
2004, Dec. 25.204	1.62	LCO40	<i>r</i>	22.19 ± 0.14
2004, Dec. 25.232	1.65	LCO40	<i>i</i>	21.82 ± 0.07
2005, Jan. 8.339	15.75	Keck/LRIS	<i>R</i>	24.5 ± 0.3
2005, Jan. 25.333	32.75	Keck/NIRC	<i>K_s</i>	> 22.0
GRB 050117a				
2005, Jan. 18.146	0.61	P200/WIRC	<i>K_s</i>	> 18.5
GRB 050124				
2005, Jan. 25.500	1.02	Keck/NIRC	<i>K_s</i>	19.66 ± 0.06
2005, Jan. 25.486	1.04	Keck/NIRC	<i>J</i>	20.90 ± 0.05
2005, Jan. 26.472	1.99	Keck/NIRC	<i>K_s</i>	20.63 ± 0.18
2005, Jan. 26.486	2.01	Keck/NIRC	<i>J</i>	22.04 ± 0.17
GRB 050126				
2005, Jan. 26.682	0.18	Keck/NIRC	<i>K_s</i>	19.45 ± 0.17

NOTE.—Ground-based optical and NIR observations of the four bursts discussed in this paper. The columns are (left to right): (i) UT date of the observation, (ii) time since the burst, (iii) telescope/instrument, (iv) filter, and (v) observed magnitude (not corrected for Galactic extinction). Limits are 3σ .

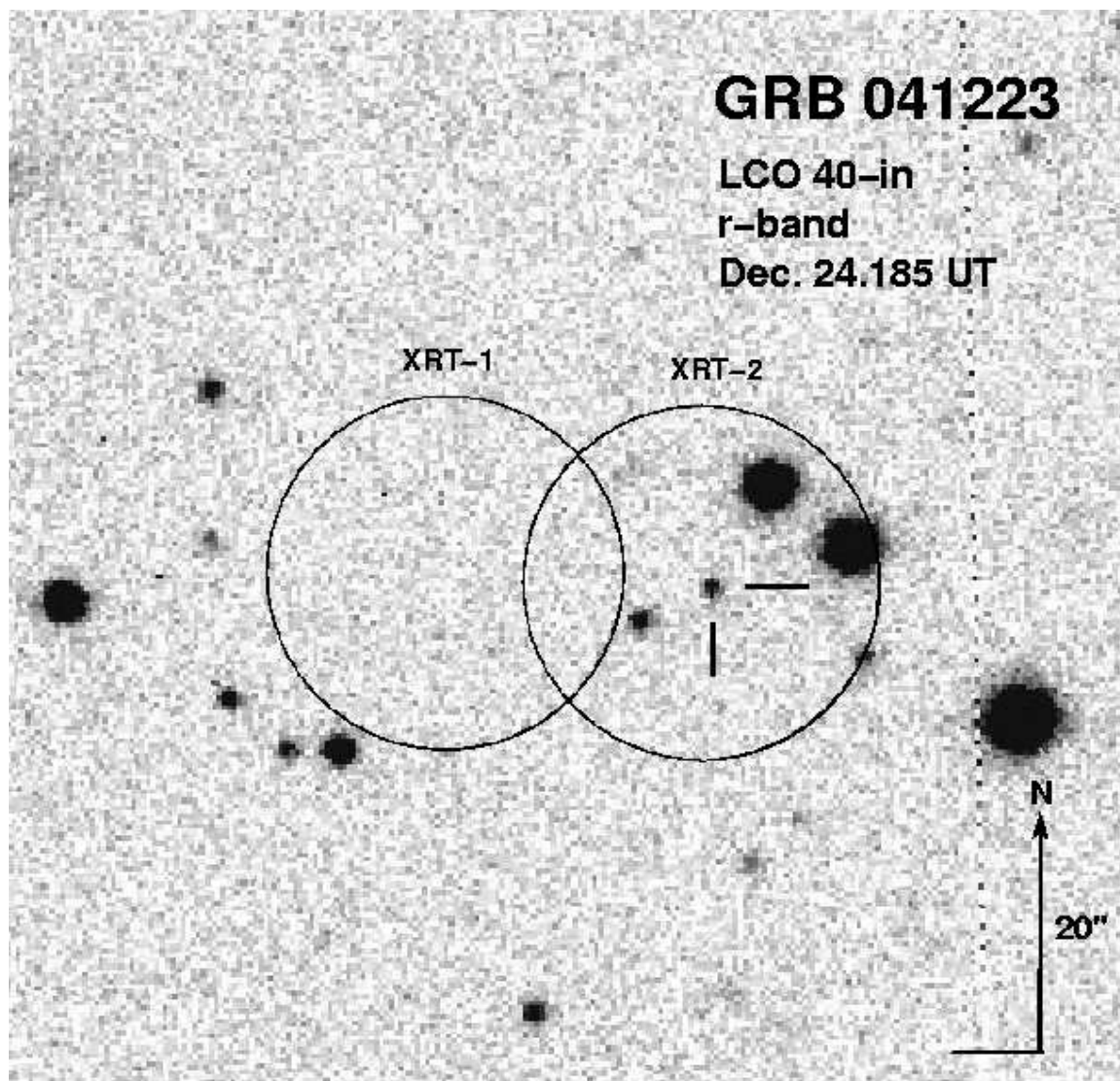


FIG. 1.— The field centered on the position of the optical afterglow of GRB 041223 (crosshairs) imaged in the r -band with the LCO 40-in telescope on Dec. 24.185 UT (14.4 hrs after the burst). Also shown are the initial (XRT-1) and revised (XRT-2) $15''$ radius error circles from *Swift*/XRT.

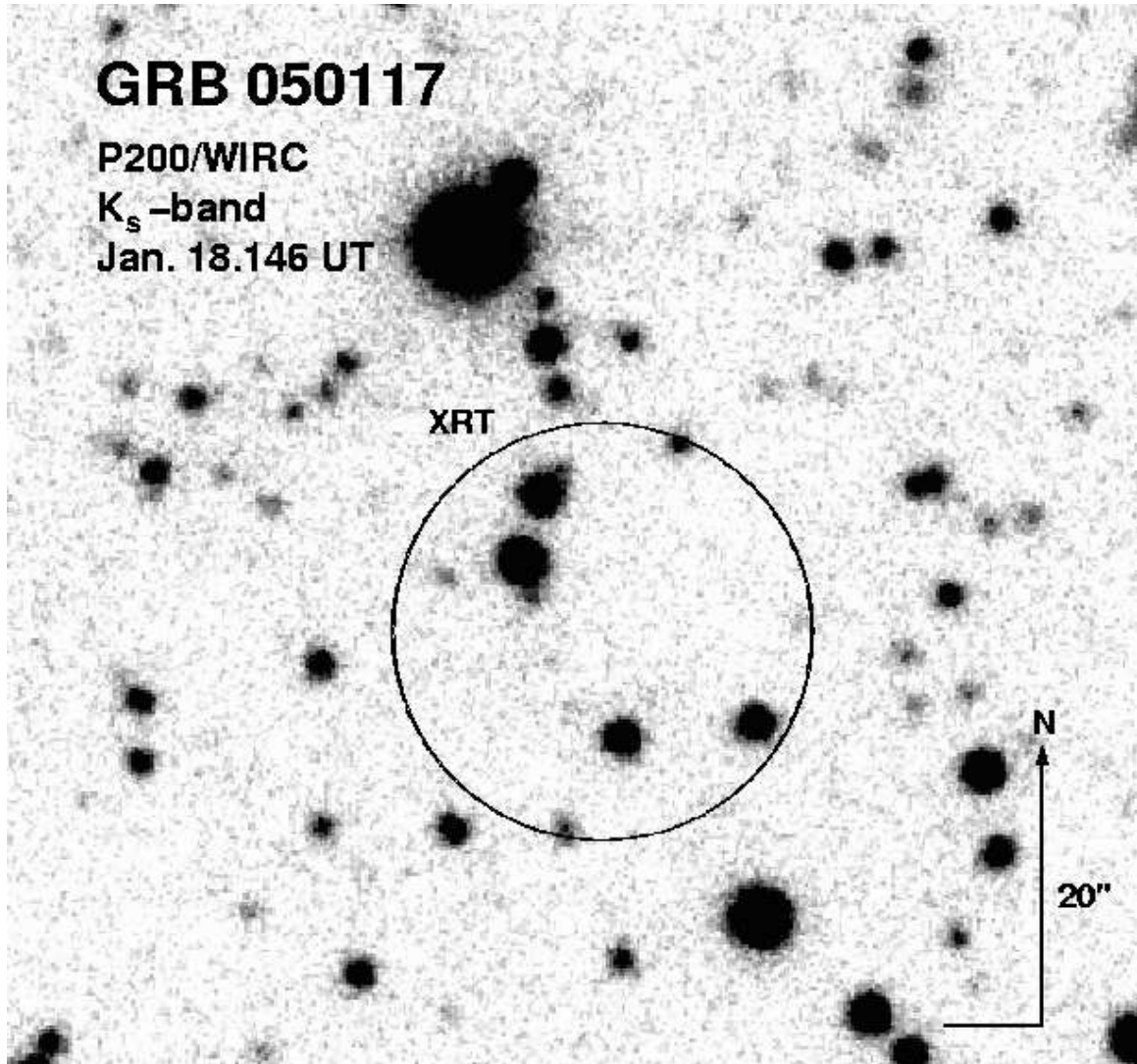


FIG. 2.— The field centered on the XRT position of GRB 050117a imaged in the K_s -band with WIRC on the Palomar 200-in telescope on Jan. 18.146 UT (14.6 hrs after the burst). Also shown is the $15''$ radius XRT error circle.

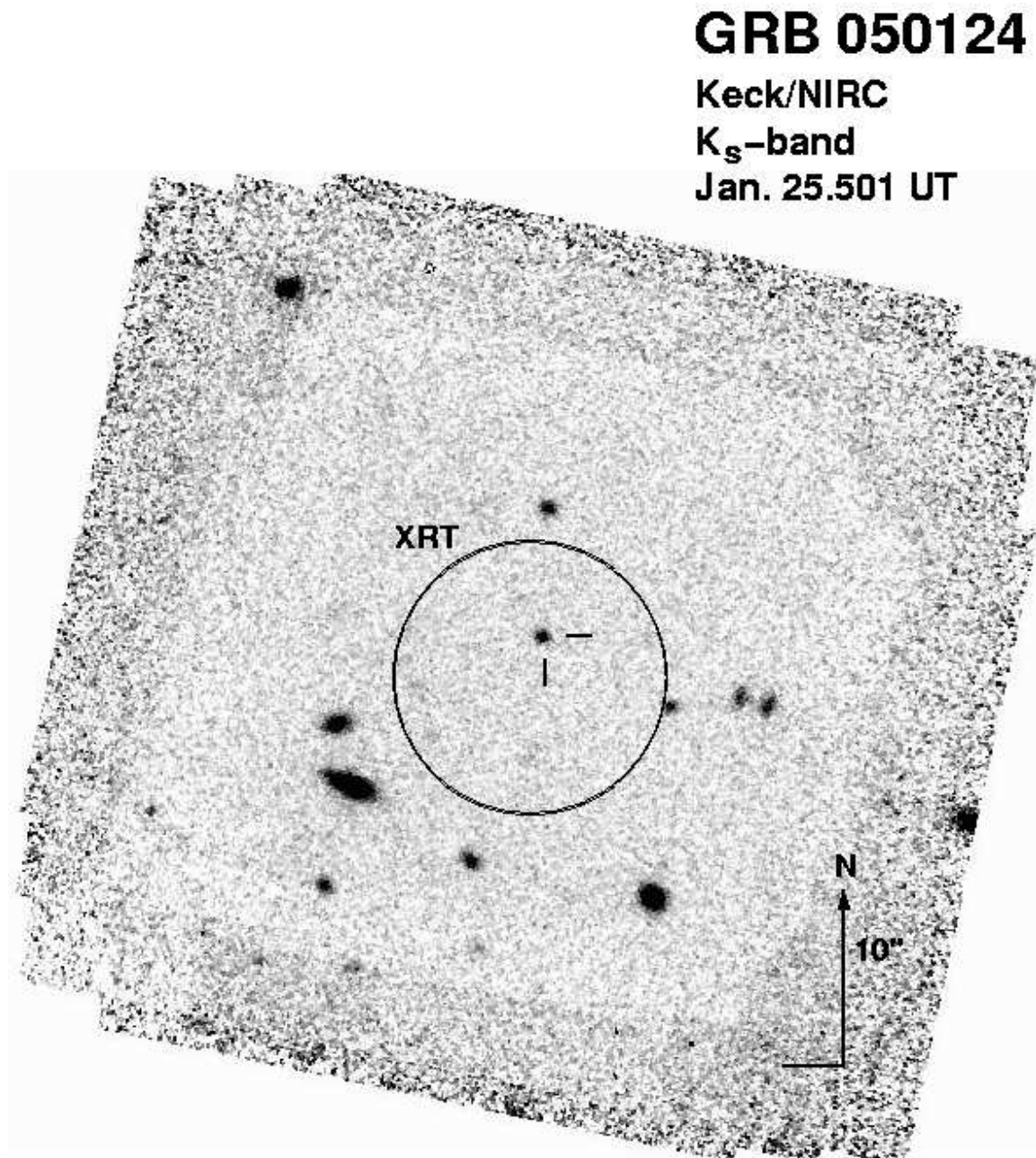


FIG. 3.— The field containing the position of the NIR afterglow of GRB 050124 (crosshairs) imaged in the K_s -band with NIRC on the Keck I 10-m telescope on Jan. 25.501 UT (24.5 hrs after the burst). Also shown is the revised *Swift*/XRT $8''$ radius error circle.

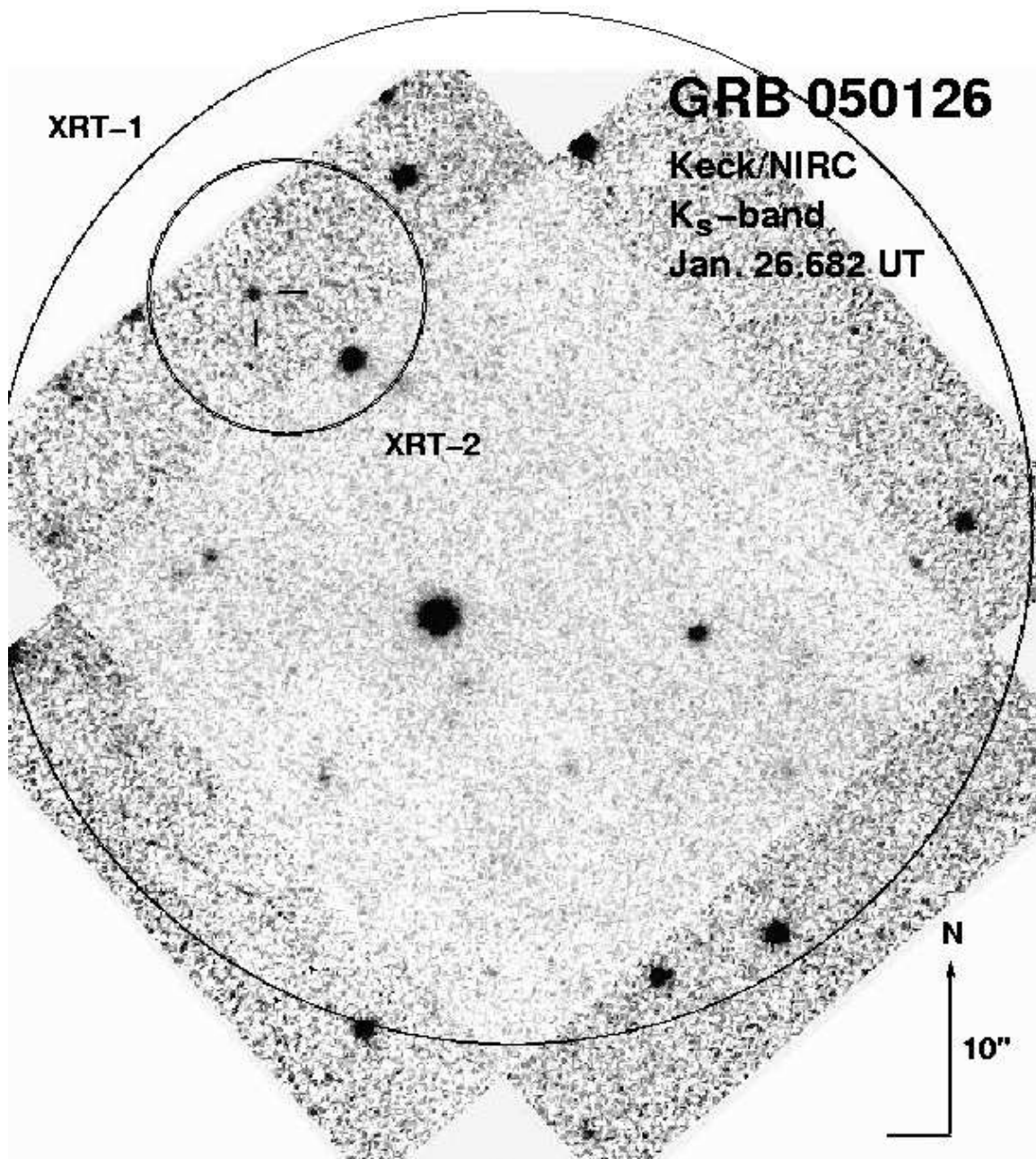


FIG. 4.— The field containing the position of the NIR afterglow of GRB 050126 (crosshairs) imaged in the K_s -band with NIRC on the Keck I 10-m telescope on Jan. 26.682 UT (4.4 hrs after the burst). Also shown are the initial (XRT-1) 30'' radius *Swift*/XRT error circle, and the revised (XRT-2) 8'' radius error circle.

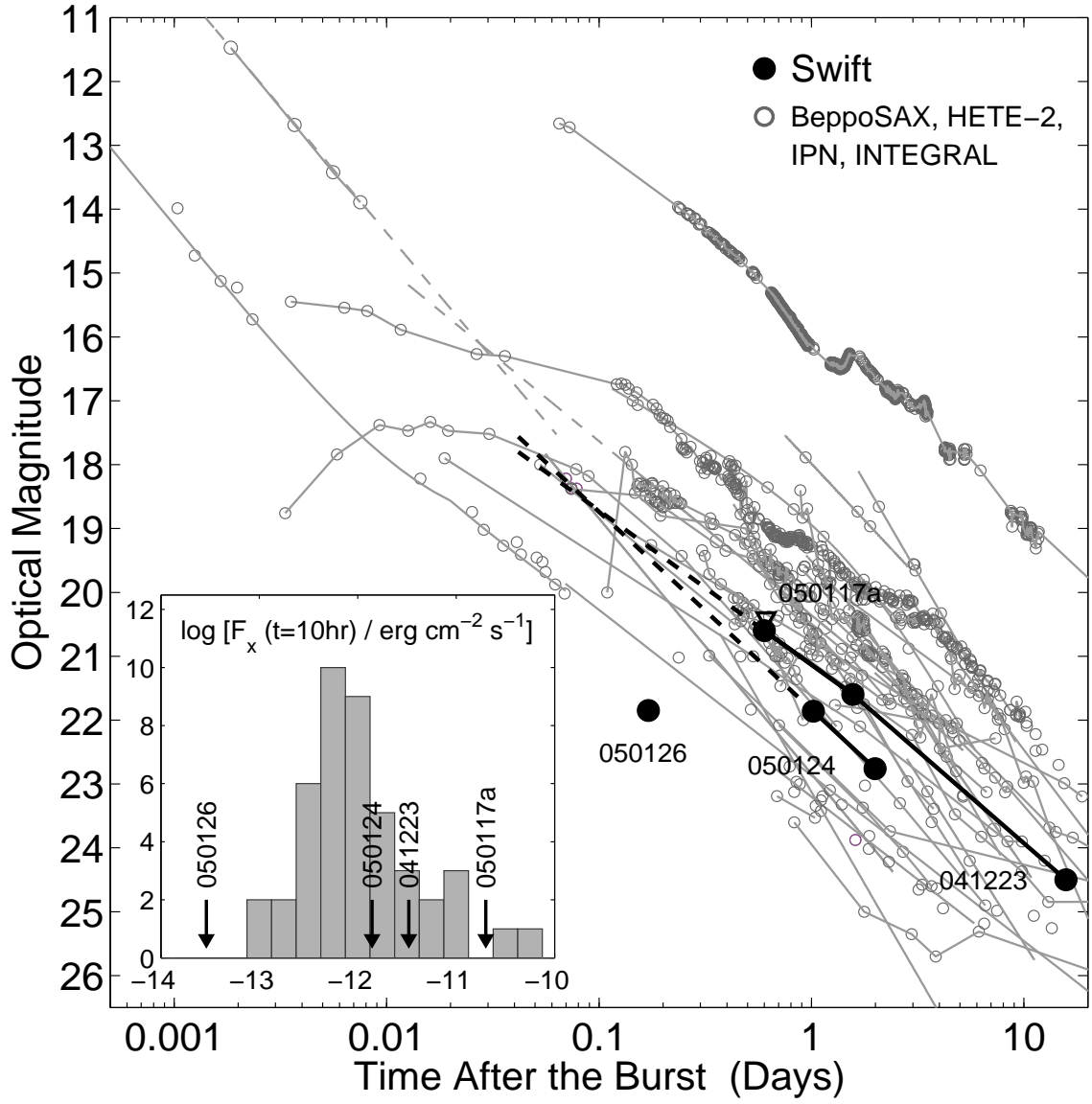


FIG. 5.— Optical light curves of the *Swift* bursts discussed in this paper (and upper limit on GRB 050117a) compared to the sample of afterglows detected and studied in the past seven years. We transformed the NIR flux of GRB 050124 to the *R*-band using the measured spectral index, and that of GRB 050126 assuming a typical index of $\beta = -0.6$. The *Swift* afterglows are fainter than about 75% of the known afterglow population. Their detection was due to the small error circles from XRT and searches with large telescopes. The inset shows the distribution of X-ray fluxes at $t = 10$ hrs after the burst for the XRT bursts (using measured temporal decay indices or assuming the typical $\alpha_x = -1.3$) compared to the sample of Berger, Kulkarni & Frail (2003). Three of the four afterglows are typical of the general population, but the afterglow of GRB 050126 is the faintest detected to date, in agreement with the faintness of the possible NIR afterglow. We note that the X-ray emission for GRB 050117a is contaminated by the prompt emission and should be considered as an upper limit.

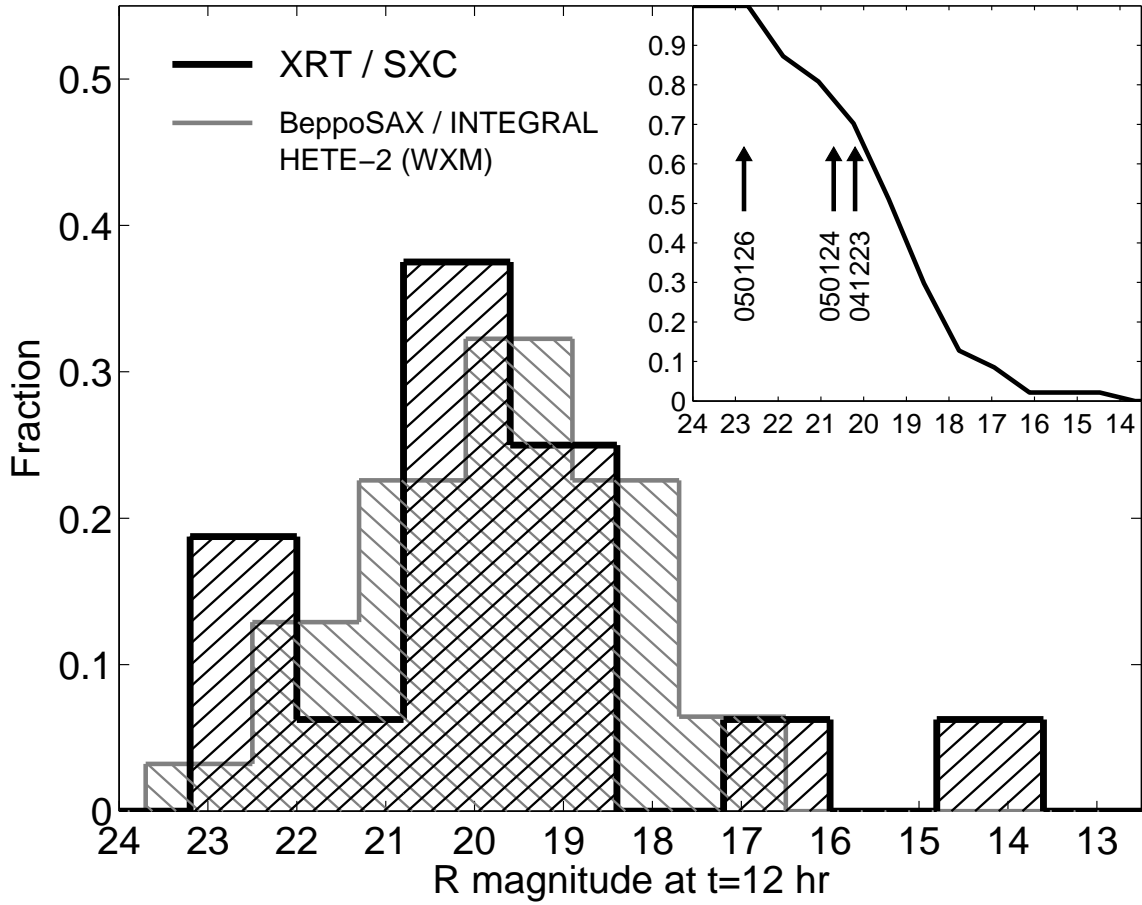


FIG. 6.— Distribution of *R*-band magnitudes normalized to 12 hrs after the burst for the XRT+SXC sample (black; 16 afterglows) compared to all other optical afterglows (gray; 31 afterglows). The afterglow detection rate for the XRT+SXC sample is about 90% suggesting that the fraction of dust-obscured (“dark”) GRBs is small. The inset shows the cumulative distribution for all afterglows discovered prior to *Swift* along with the three afterglows discussed in this paper. The *Swift*/XRT bursts are fainter than about 75% of all afterglows localized to date. In the past, these may have been designated as dark.